

Using Eclipse to Probe Physical Conditions Along the Jets in the X-Ray Binary SS 433

Xinyi Liu¹ Herman Marshall² Dipankar Maitra¹
Michael Nowak² Norbert Schulz³ Diego Altamirano⁴
Jack Steiner² and the NICER team

¹Wheaton College, MA

²MIT Kavli Institute, MA

³Washington University at St. Louis, MO

⁴University of Southampton, England

Rhode Island Space Grant Spring Symposium, 2019

Outline

1

Introduction

- SS 433 system
- Observation strategy and data acquisition

2

Investigate two jets with the X-ray spectrum

- Spectral Analysis
- Data Analysis

3

Discussion

4

Reference

SS 433 system

An X-ray Binary system

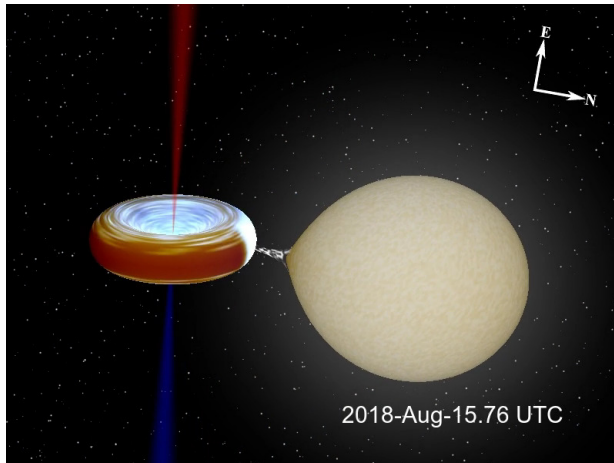


Figure: The orbital motion of a binary system

SS 433 system

Jet Precession

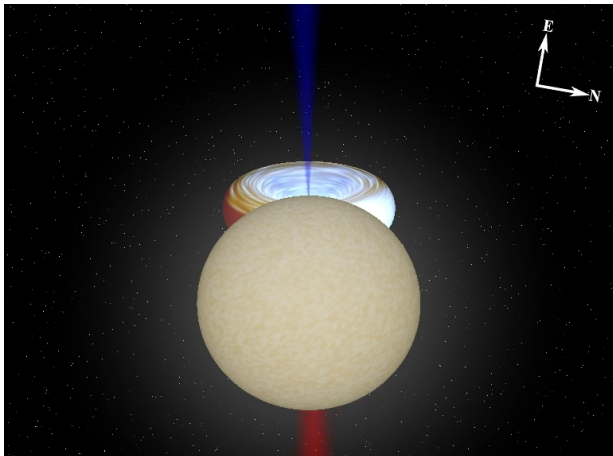
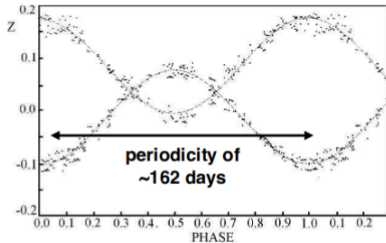
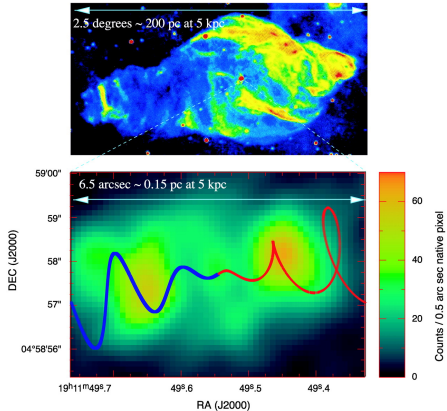


Figure: Jet precession

Moving Lines and the Surrounding Nebula



(a) The periodic redshifts of both jets (GRAVITY et al., 2017)



(b) SS 433 jet precession cycle and the surrounding W50 radio nebula (Migliari et al., 2002)

Motivations

Fundamental questions in high-energy astrophysics

- Jet's launching mechanism
- The evolution of the physical conditions along the jet
- The nature of the compact object

Chandra Telescope

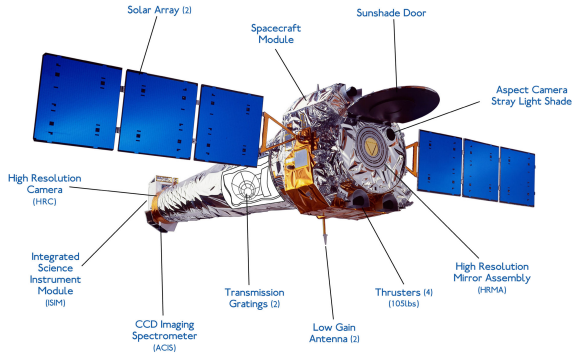


Figure: The Chandra Telescope with main components labeled (Harbaugh, 2017).

Observation Strategy

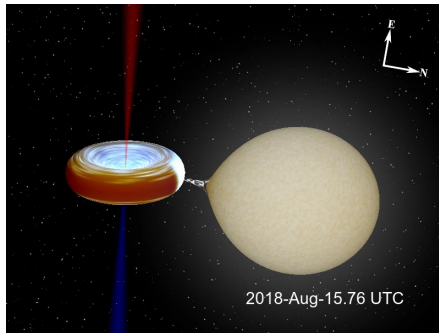


Figure: The orbital motion of ss 433 during our observation

- A short observation (20 ksec) 3 days before the eclipse.
- A long observation (100 ksec, split into 5 parts) starting in the middle of the eclipse.

Fitting Method

Phenomenological Fitting Model (Houck and Denicola, 2000)

- **Absorbed Power Law**

$N(E) = KE^\alpha$, where K is photons/keV/cm²/s at 1 keV and α is the photon index.

- **Gaussian Emission Lines**

$N(E) = K \frac{1}{\sigma\sqrt{2\pi}} \exp\left(-\frac{(E - E_l)^2}{2\sigma^2}\right)$ where K is the total photons/cm⁻²/s in the line, E_l is line energy in keV and σ is line width in keV.

The Phenomenological Fitting

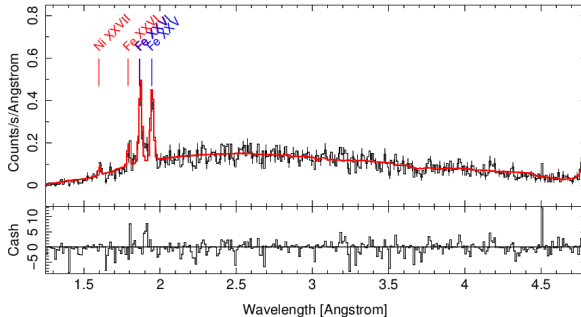


Figure: The phenomenological fitting for the spectrum of the short and long observation.

The Phenomenological Fitting

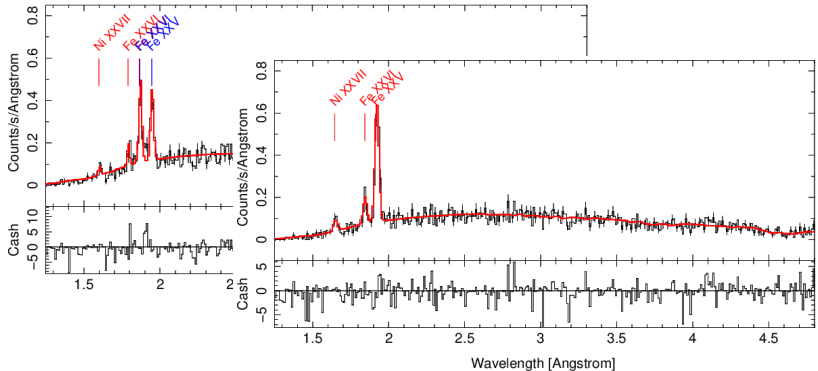


Figure: The phenomenological fitting for the spectrum of the short and long observation.

The Phenomenological Fitting

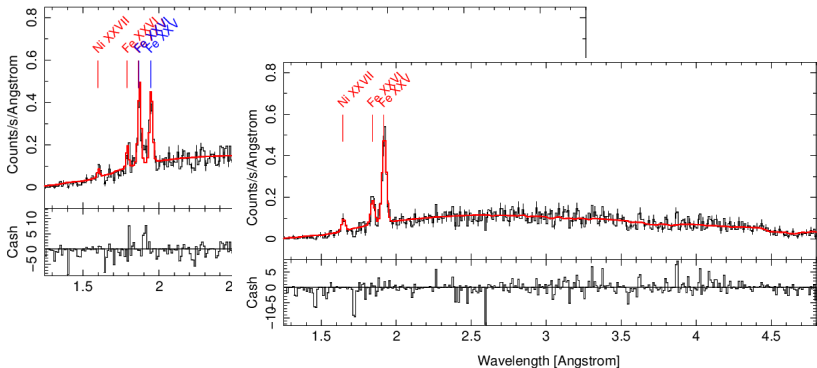


Figure: The phenomenological fitting for the spectrum of the short and long observation.

The Phenomenological Fitting

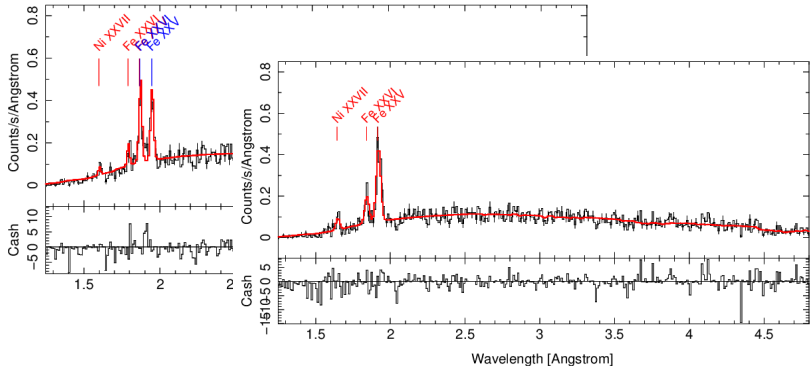


Figure: The phenomenological fitting for the spectrum of the short and long observation.

The Phenomenological Fitting

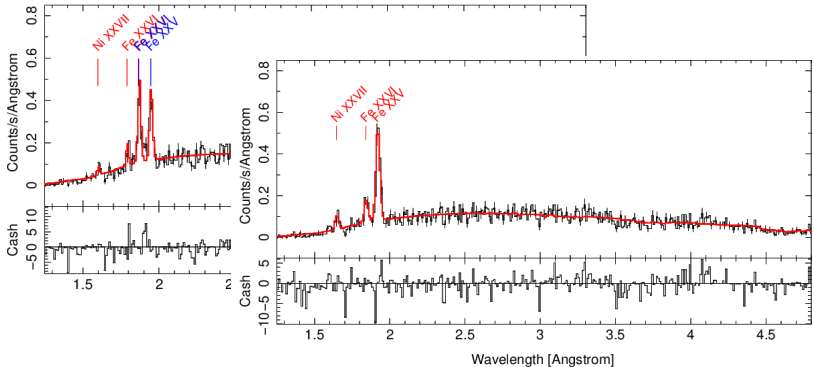


Figure: The phenomenological fitting for the spectrum of the short and long observation.

The Phenomenological Fitting

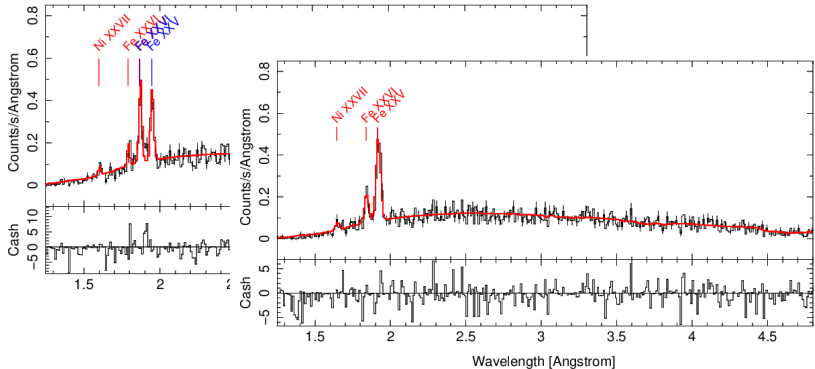


Figure: The phenomenological fitting for the spectrum of the short and long observation.

Plasma Model

Plasma

Plasma is an electrically neutral medium that consists of a mixture of an electron gas and an ion gas.

Plasma Model

Four-temperature plasma model with parameters of temperatures, metal abundance, redshift, turbulent velocity and normalization (Marshall et al., 2002).

Spectral Analysis

Plasma Model Fitting

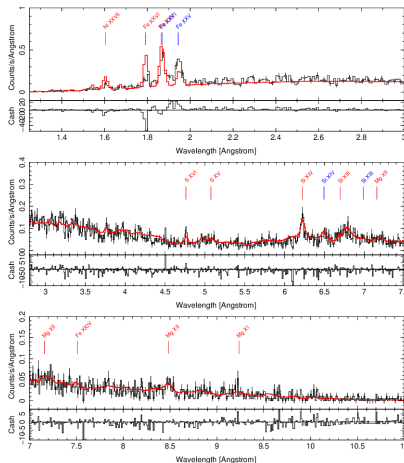


Figure: Plasma model fit to the short observation

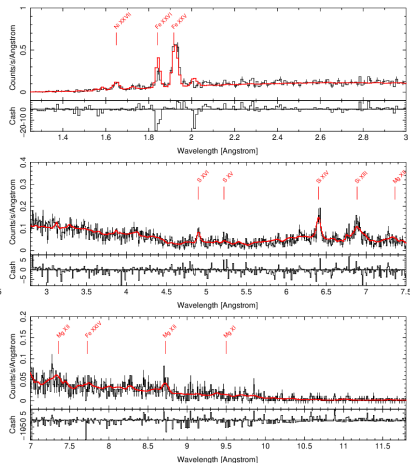


Figure: Plasma model fit to the first part of the long observation

The Redshift Variations over the Short and Long Observations

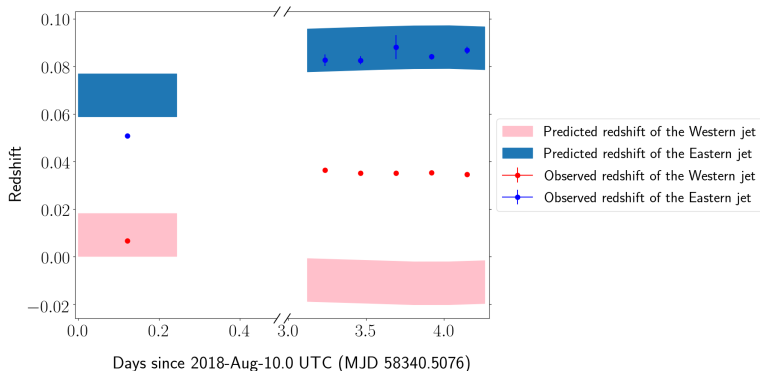


Figure: The predicted (Maitra et al., 2018) and observed redshifts values (with error bars) over the short and long observations of the western and the eastern jets.

The Line flux Variations over the Short and Long Observations

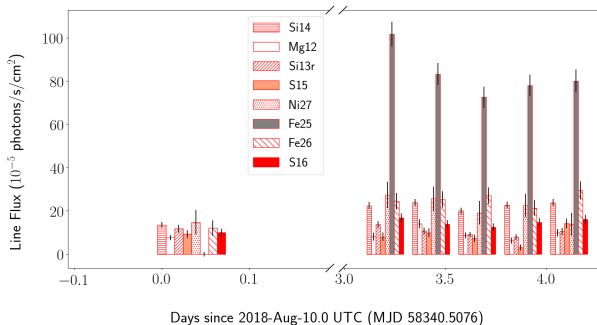


Figure: The flux variations of 8 most notable emission lines from the Western jet over the short and long observations

The Line flux Variations over the Short and Long Observations

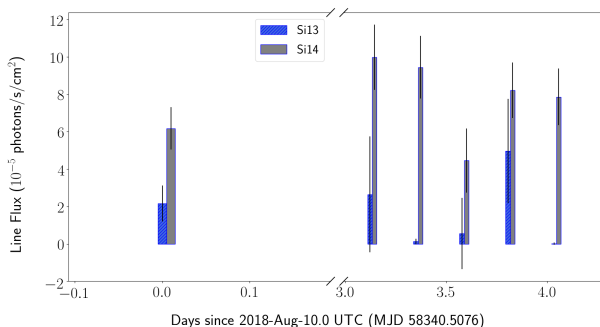


Figure: The flux variations of Si13 and Si14 emission lines from the Eastern jet over the short and long observations. Lines that disappear (Fe 25 and Fe 26) in the long observation are excluded in this graph.

The Line flux Variations over the Short and Long Observations

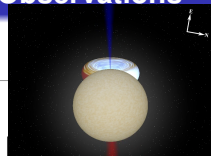
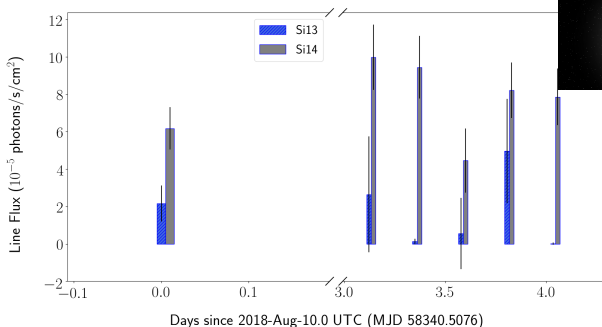


Figure: The flux variations of Si13 and Si14 emission lines from the Eastern jet over the short and long observations. Lines that disappear (Fe 25 and Fe 26) in the long observation are excluded in this graph.

Data Analysis

The Variations of Normalization and Photon Index of the Powerlaw Photon Spectrum

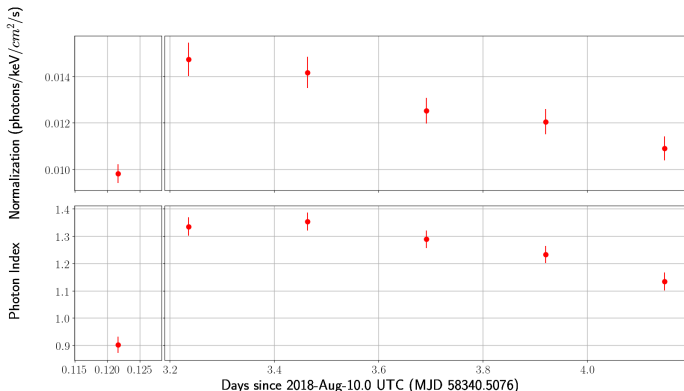


Figure: The change of normalization and photon index of the powerlaw photon spectrum over the long and short observation.

Discussion

- Why there is a large discrepancy between the observed and predicted redshift values of the Western jet over the long observation?
- Why there are more lines from the Western jet than the Eastern jet?
- What can change of line fluxes tell?
- What portions of jets are blocked by the companion during eclipse?

Acknowledgements

Many thanks to

- Chandra X-ray Center/Smithsonian Astrophysical Observatory
- NASA Rhode Island Space Grant Consortium

References

- Harbaugh, J. (2017). Chandra spacecraft and instruments.
- Houck, J. C. and Denicola, L. A. (2000). . In Manset, N., Veillet, C., and Crabtree, D., editors, *Astronomical Data Analysis Software and Systems IX*, volume 216 of *Astronomical Society of the Pacific Conference Series*, page 591.
- Maitra, D., Marshall, H., Nowak, M., and Schulz, N. (2018). What is where? using eclipses to probe physical conditions along the jet in ss433.
- Marshall, H. L., Canizares, C. R., and Schulz, N. S. (2002). The high-resolution x-ray spectrum of ss 433 using the chandra hetgs. *The Astrophysical Journal*, 564(2):941.
- Migliari, S., Fender, R., and Méndez, M. (2002). Iron emission lines from extended x-ray jets in ss 433: Reheating of atomic nuclei. *Science*, 297(5587):1673–1676.